Journal of Theoretical and Applied Information Technology
30th April 2020. Vol.98. No 08

ISSN: 1992-8645 www.jatit.org E-ISSN: 1817-3195

FEASIBILITY OF EXTERNAL RADIOTHERAPY DOSE ESTIMATION IN HOMOGENOUS PHANTOM USING MONTE CARLO MODELING

[1]ZAKARIA AITELCADI, [1,2]AHMED BANNAN, [1]REDOUANE EL BAYDAOUI, [1]MR MESRADI, [1]ABDELLAH HALIMI, [1]SAAD ELMADANI

[1]Laboratory of Sciences and Health Technologies, High Institute of Health Sciences, Univ Hassan 1, B. P. 577, 26000 Settat, Morocco
[2] Majorelle Oncology Center Marrakech, Morocco

E-mail : [1]z.aitelcadi@gmail.com, [1,2]ahmedbannan92@gmail.com, [1]redouane.elbaydaoui@uhp.ac.ma
[1]mesradi_reda@yahoo.fr, [1]halimiabdellah@yahoo.fr, [1]saad.elmadani@uhp.ac.ma

ABSTRACT

This work relates to the study of a Varian Clinac IX 6MV photon beam from measurement and simulation of tree fundamental functions, the Percentage Depth Dose (PDD), the Dose Profile (DP) and the collimator scatter factor (Sc). Simulations were performed using the recent version of the Monte Carlo simulation code GATE (v8.1). It was used to model the geometry of the accelerator head, optimize the configuration of the electron source and calculate the dose for different field sizes (3x3 cm^2, 4x4 cm^2, 6x6 cm^2, 8x8 cm^2, 12x12 cm^2, 15x15 cm^2, and 20x20 cm^2). The Geometry was modeled using the parameters given by the Varian manufacturer under agreement. To generate the bremsstrahlung photon beam, an electron source with a mean energy of 5.8MeV and a half-width of 1mm was used, its parameters were determined for a relative dose difference between 2% and 2.5% for PDD and DP respectively. After using the simulation splitting, the variance reduction and the phase space techniques, the computing time consumed by the simulations was reduced by a factor of 160. Otherwise Good agreement within 1% was found for the Collimator scatter factor (Sc). The presented results show that the GATE model of Varian Clinac IX 6MV photon beam might be used to evaluate the systematics dosimetric errors and for clinical applications using the recent treatment technics.
Keywords: GATE*; Monte Carlo; Varian; HPC; Dosimetry; Collimator Scatter Factor; Linear Accelerator.*

1. INTRODUCTION

In radiotherapy, the accuracy of the dose calculation for the treatment planning is paramount. Among the algorithms for calculating dose distributions, the Monte Carlo method is potentially the most accurate, if the radiation source and the patient are completely modeled [1].

Indeed, the advantage of the Monte Carlo (MC) methods is its ability to precisely simulate the transport of radiation in the accelerator treatment head in homogeneous and heterogeneous anatomical structures of the patient. The attenuation and scattering effects of irradiation beam can be accurately described. Similarly, the effects of disruption dose observed with low density tissues can be accounted by accurate dose calculation [2,3].

Different research group have been focused on the study of the absorbed dose in external beam radiotherapy using a Varian Clinac IX 6MV photon beam by several Monte Carlo (MC) simulation codes (MCNP [4], EGS [5] and Geant4[6]). In this work, the validation of the Varian Clinac IX for a 6MV photon beam has been studied using the latest version of Monte Carlo simulation GATE V8.1 [7] code. The key factor in dose simulation is the precision of results that depend widely on the configuration of the electron source, the accelerator head geometry based on (primary and secondary collimators, flattening filter), the atomic density of the target and the techniques used to reduce the calculation time.

In this study our approach was first to configure the electron source by applying the relative dose difference method [8] with a tolerance of 2%, comparing the simulated dosimetric functions (Percentage Depth Dose (PDD) and the Dose Profile (DP)) with the measured ones. Secondly, we optimized the computing time using an HPC

ISSN: 1992-8645 www.jatit.org E-ISSN: 1817-3195

workstation [9] using the simulation splitting, the variance reduction and phase space techniques. Finally, we validated the Varian Clinac IX by comparing the simulated curves of the three functions, PDD, DP and the collimator scatter factor (Sc) to those measured in a homogeneous phantom with a dimension of 50x50x50cm3 for different clinically available field sizes (3x3cm2, 4x4cm2, 6x6cm2, 8x8cm2, 12x12cm2, 15x15cm2, and 20x20cm2) using two detectors, a cylindrical ionization chamber and a diode dosimeter.

2. MATERIAL & METHODS

2.1 Measurements

Measurements have been carried out on Majorelle Oncology center in Marrakech. The accelerator used is the Varian Clinac IX (Varian Medical, System, Alto Pal, Calif.) for a 6 MV photon mode. To estimate the dose distribution (PDD and DP), a 3-axis water scanning phantom, called DoseView 3D was used; it can scan a maximum field size of 50 × 50 cm^2 and a depth of 41 cm with an accuracy of 0.1 mm in all directions; the distance between the phantom surface and the beam source (SSD) was fixed at 100cm. The dose in the phantom was measured with two types of detectors that present a major interest in radiotherapy. A cylindrical ionization chamber (Exradin A28 from standard imaging USA) and a diode dosimeter (micro-silicone PTW from Germany), with a sensitive volume of 0.125cm^3, 0.03cm^3 respectively was exploited. Because of its small volume, the diode dosimeter was used to measure the dose function (PDD and DPs) for the smaller field sizes (< 4x4cm^2). While the cylindrical ion chamber was used for the other filed sizes (4x4 cm^2, 6x6 cm^2, 8x8 cm^2, 12x12 cm^2, 15x15 cm^2, and 20x20 cm^2). The spatial resolution parameter (in x and y directions) was fixed at 0.1mm in the penumbra region and at 1 mm elsewhere for DPs. For PDDs we have choose a step of 0.1 mm for depths between 0cm and 5cm and 1mm for depths greater than 5 cm. The collimator scatter factor (Sc) may be defined as the ratio of the dose at 5cm of depth for a given field size (3x3, 4x4, 6x6, 8x8, 12x12, 15x15 and 20x20 cm^2) to that for the reference field size of 10 × 10 cm^2.

2.2 Monte Carlo simulations

2.2.2 Modeling of Linac IX head geometry

In this work, the MC code GATE was used to model all components of the accelerator head (target, primary collimator, flattening filter, mirror and jaws). The technical information of the different compositions (geometries and materials) of the accelerator head of Clinac IX were provided by the manufacturer of the machine (Varian Medical Systems) with an agreement [10]. A screen shot of the modeled accelerator by GATE is shown in Figure 1.

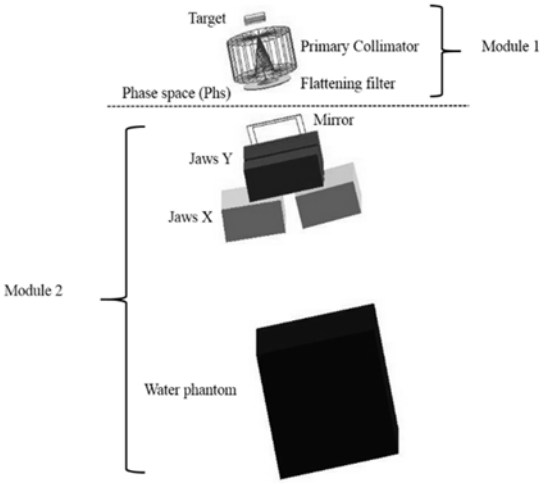

Figure 1: Illustration of GATE model of Varian Clinac IX

2.2.3 Modeling the electron source

Modeling an electron source consists to determine the mean energy of the electrons and their trajectories [11]. In fact, an increase of 0.2 MeV in mean energy and a slight divergence of the electron beam induces a direct effect on the dose rate at PDD and DP [12,13]. For an appropriate configuration of the electrons source, we applied the method of Cho et al. [8]. This method consists to evaluate the relative dose difference between an experimental value and a theoretical reference value according to the equation (1), where D_c represents the calculated absorbed dose and D_m is the measured one (reference). In these conditions, the difference in dose must be less than 3% in the build-up region and the difference must be less than 1% for the majority of depths going from the depth that corresponds to the maximum dose (D_{max}) to 30 cm.

$$RDD\ (\%) = 100 * \frac{D_c - D_m}{D_m} \qquad (1)$$

To apply this method, several dose calculations (PDD) were performed in a 50 × 50 × 50 cm^3 water phantom, with a field size of 10 × 10 cm^2 at the isocenter. The GATE dose calculations were performed with a DoseActor attached to the water phantom [14]. The output dose distribution was saved in a binary file (hdr/img). To determine the mean energy of the initial electron beam, we have calculated the parameter "σ" which is the average of differences between measured and simulated PDD. For all PDDs correspond to an energy beam range from 5 to 6 MeV with an increment of 0.2 MeV and

ISSN: 1992-8645 www.jatit.org E-ISSN: 1817-3195

an energy sigma equal to 3% of E, the absolute maximum difference (σ_{max}) [8] was calculated. Moreover, once the mean energy of the electron source is fixed, we varied the parameter full width at half maximum (FWHM) of the beam spatial distribution, by an increment of 1 mm starting from 1 mm to 4 mm, until the simulated DPs better fit with measured ones [15].

2.2.4 Physics Models

GATE V8.1 version contains different "sets" of electromagnetic (EM) process models based on theoretical calculations and experimental data. In this study, we considered three EM process: Standard [7-16], Livermore [7-16-17] and Penelope [7-16] model. The Standard model was developed for high energy physics experiments covering an energy range from 1 keV to 100 TeV. While, Livermore and Penelope are two models that take into account the "LowEnergy" models by covering energies lower than those of the standard model. They can reach energies of 250 eV for processes (photoelectric and Compton) and they allow to take into account physical processes such as fluorescence and Auger electrons. In this work, the process to choose the appropriate physic model was determined by performing simulations with the three physics models, using the electron source configured and applying the relative dose difference method to compare the calculated and measured dose distributions (PDD and DP). The suitable model for our application, was the one corresponding to a minimal relative difference and a low computation time.

2.2.5 Clustering and CPU timing

GATE calculations were performed on a cluster named HPC-MARWAN located at CNRST (RABAT) and consists of 19 nodes with 760 cores, a memory of 5.2 TB, 108 TB of storage and 2 GPU cards. These nodes are interconnected by a very low latency network at 100 Gbps, which optimizes performance for parallel calculations [9]. The need of a huge computation time by MC methods strongly push to use many tools to reduce as much as possible the computation time without biasing the final result. In the literature, several techniques have been introduced, the Splitting and Russian Roulette [18], a cut-off threshold [19], the KillActor and the phase space (Phs) [20].

In this work, in the variance reduction techniques a splitting factor of 100 was selected, and 1 mm was assigned to the energy cut (corresponds to 1/5 of the voxel dimension). The Stepfunction parameter [19] was fixed at 0.1 mm. Moreover, Cutoff energies was fixed respectively at 350 keV for electrons positrons and 5 KeV for photons.

To accelerate the simulations, a splitting script was introduced to divide the simulation into 1000 jobs running in parallel. The calculation time was reduced by a factor of 50% passing from 3200 without splitting to 1600 hours after splitting.
To more minimize the computing time, the Phase space (Phs) technique was used to divide the geometry into two parts, dependent part (module 2) and independent part (module 1) (Figure 1). In this work, the phase space was modeled as a cylinder with 10 cm of diameter and a thickness of 1 nm in the z direction and is located at 7 cm above the secondary collimator or jaws Y.

The Simulations were simplified by considering only the dependent part and by taking the Phs as a beam source. The calculation time was reduced with a gain factor of 160 (45h for module 1 and 20h for module 2). Table 1 summarizes the results of our study of minimize the consumed computing time. In addition, GATE provide a parameter called "setMaxStepSizeInRegion" for electrons that allows to limit the maximum step for a particle in a region. For that reason, we have examined different values of this parameter by varying it from 10 to 50µm with a step of 10µm to have a value assigned with the recommended value of cut energy and taking into consideration a reasonable calculation time [20]. Table 2 shows the calculation time for each value (Phs as a source).

Table 1: CPU Timing For The GATE Modeled Varian Clinac Ix.

VARIAN Clinac IX geometry	CPU (h)
Whole geometry (Module 1 + Module 2)	3200
In-house script (1000 jobs)	1600
Phase space: • Module 1 • Module 2	 45 20

Table 2: CPU Timing For Different Values Of "Setmaxstepsizeinregion" Applied In Electrons.

value of "setMaxStepSizeInRegion" (µm)	CPU (h)
10	30
20	20
30	48
40	53
50	59

ISSN: 1992-8645 www.jatit.org E-ISSN: 1817-3195

3. RESULTS & DISCUSSION

3.1 Electron source optimization and physic models

Electron source has been studied in terms of two parameters, the mean energy and the half-width FWHM. Optimal mean energy of electrons was found by modeling six mono-energetic electron sources with an energy equal to 5, 5, 2, 5,4, 5,6, 5, 8 and 6 MeV (Figure 2). Table 3 presents the influence of the variation of the mean energy on the differences between the simulated and measured values of the PDD, by calculating σ and σ_{max} which represents respectively the average of the differences and the absolute maximum difference. The values of σ and σ_{max}, indicated that mean energy of 5.8 MeV, that better meets the criteria given by the method of Cho et al, with σ between -1% and 1 %, σ_{max} is around 1.5%.

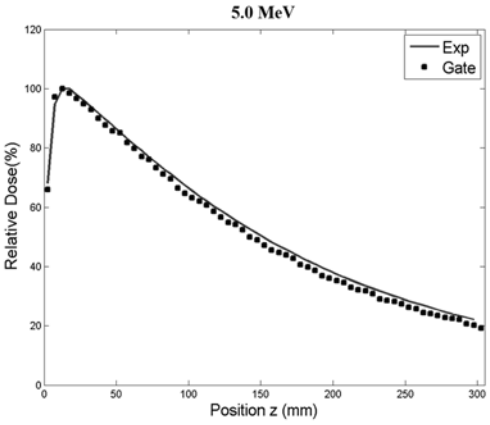

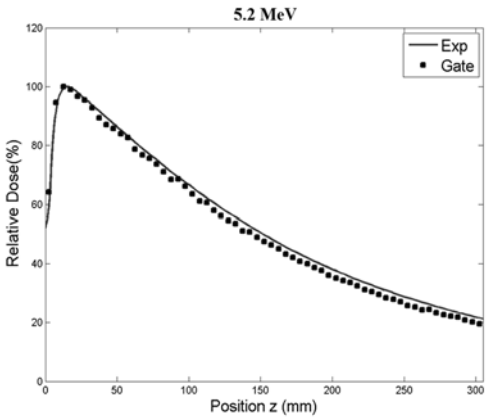

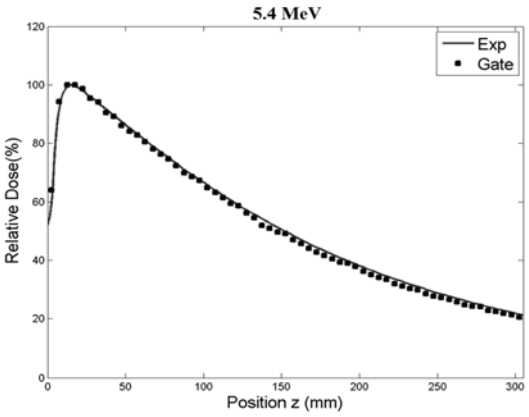

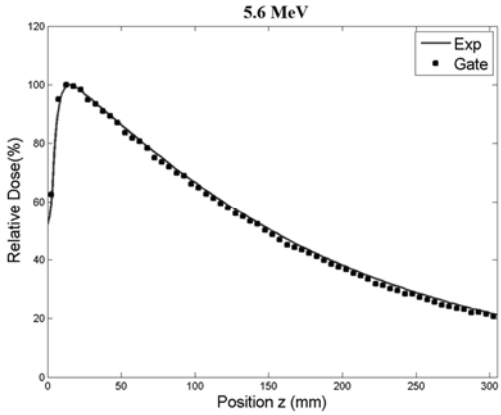

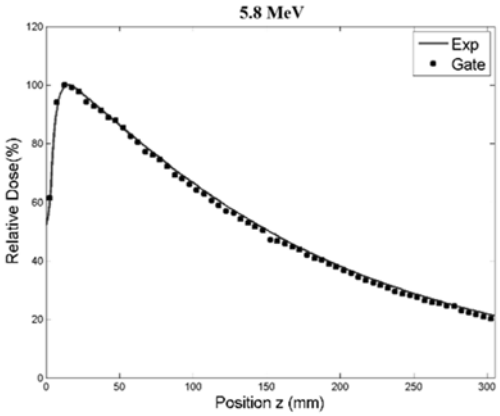

ISSN: 1992-8645 www.jatit.org E-ISSN: 1817-3195

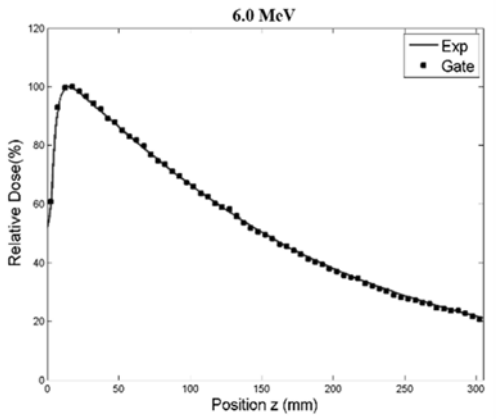

Figure 2: Simulated PDDs vs measured ones for different six energy distributions of the electron source beam, for a 10x10 cm² field size.

In addition, figure3 shows that the dose values increased by an average of 5% while the mean energy increased from 5 to 6 MeV. In fact, in the buildup region, the largest relative dose differences are found for water depths less than or equal to 0.5 cm. These dose differences are due to the contamination of electrons consists the main component of the input dose [21,22].

It consists of secondary electrons arising from the interactions of high energy photons with the accelerator head elements, and secondary electrons generated by the interactions in the air (between the exit of the accelerator head and the entry of the water phantom) at low energy. The origin of these differences is due firstly to the electrons of contamination biased by the inaccuracy of the secondary collimation modeled and secondly to an uncertainty of measurement of the higher dose in buildup region [23], caused by the high dose gradients and dimensions of the ionization chamber. At depths greater than D_{max}, the PDD increased when the mean electron energy increased. The higher mean energy of the initial electron generates a higher bremsstrahlung photonic energy in the target, which allows the photons to produce secondary electrons that penetrate the water more efficiently and can deliver their energy to deeper locations in the beam direction.

Table 3: σ And σ_{max} Results For Six Energy Distributions Of The Electron Source Beam.

Mean energy (MeV)	σ(%)	σ_{max}(%)	CPU (h)
5.0	-0.8	2.78	22
5.2	-0.51	1.88	23
5.4	-0.33	1.85	26
5.6	-0.2	1.43	22
5.8	0.04	1.22	20
6.0	0.18	1.98	27

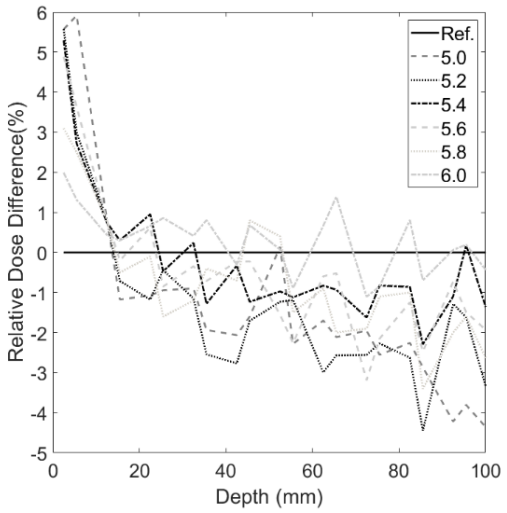

Figure 3: PDD Relative dose difference for different electron beam energy.

Optimal FWHM was found by modeling the DPs with different values from 1 to 4 mm (Figure 4). The obtained values of σ and σ_{max} presented in Table 4, demonstrates that the electron source with a FWHM value of 1 mm satisfies the criteria of comparisons with values of σ less than 1% and those of σ_{max} less than 2.5%. In addition, figure 5 shows that the initial radial distribution of the electron beam is inversely proportional to the dose values of the profile. Compared to the reference beam, the average dose difference in the horn region increased from 1.3% to 16.3%, while the radial beam width increased from 1mm to 4mm. The maximum and minimum differences in the horn were estimated respectively at 33.7% when the FWHM equal to 4mm and at 2.28% in the case of FWHM equal to 1mm.

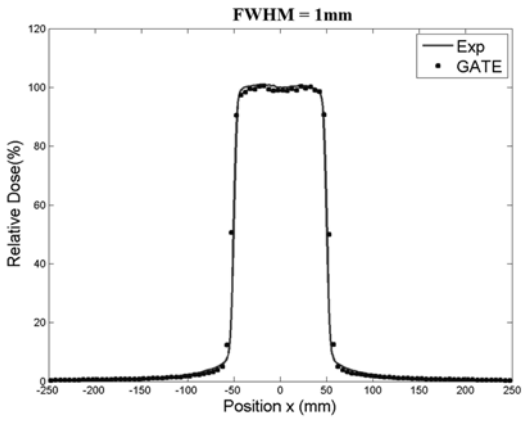

ISSN: 1992-8645 www.jatit.org E-ISSN: 1817-3195

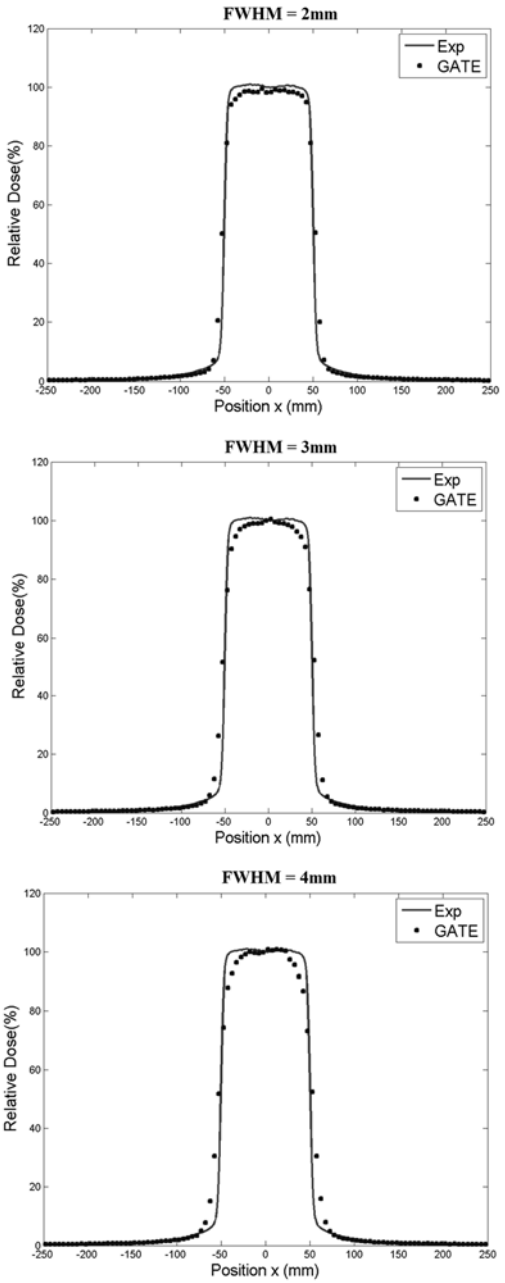

Figure 4: Simulated DPs vs measured ones for five different FWHM values of the spatial distribution of the electron source beam.

Table 4: σ And σ_{max} Results Applied To PD For Five Different Spatial Distributions Of The Electron Source Beam.

FWHM (mm)	$\lvert\sigma\rvert$(%)	σ_{max}(%)	CPU (h)
1	0.33	1.02	20
2	1.38	2.52	28
3	2.74	2.96	35
4	3.79	3.38	38

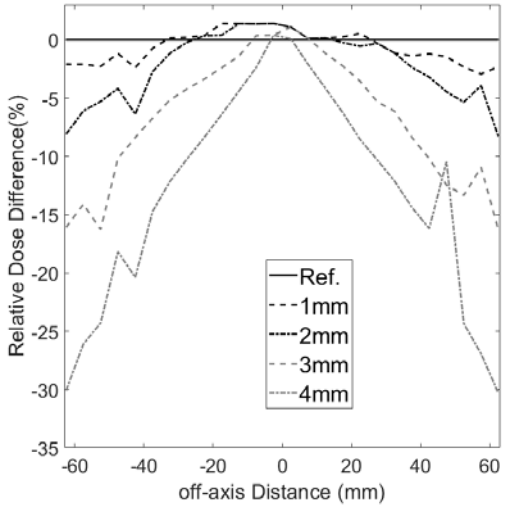

Figure 5: DP Relative dose difference for different electron beam energy.

The results of using different physics models (Figure 6) shows that the minimum value of σmax (Table 5) is observed when applying the standard model, contrary to Penelope model, where a maximum value of σmax was calculated (Table 5). Moreover, we observe that both Penelope and Livermore models consume more CPU time compared to Standard model which due to the range of energy of each model. The application of Standard model accelerates the simulation, passing from 38 hours in the case of Livermore to 20 hours [7-16-17].

Table 5: σ And σ_{max} Results Applied To PDD And DP For Three EM Physics Models.

EM Models	PDD	DP	PDD	DP	CPU
	$\lvert\sigma\rvert$ (%)		σ_{max} (%)		(h)
Standard	0.04	0.33	1.22	1.02	20
Penelope	1.33	1.99	2.92	3.55	29
Livermore	1.08	1.53	1.82	2.63	38

3.2 Validation of Varian Clinac IX

In this work, based on the comparison of the simulated PDDs and PDs with measurements, the obtained optimal electron beam was characterized by a mean of energy 5.8MeV with standard deviation of 0.168 MeV (3% of 5.8MeV) and a 1mm of FWHM of its spatial distribution.

Using this configuration, a comparison between the simulated PDD and DPs with measurements were presented in Figures 7 and 8 respectively. Where PDD curves were normalized to D_{max}. Table 6 exhibits the basing of PDD on the criteria given by Cho and al. It shows a good

ISSN: 1992-8645 www.jatit.org E-ISSN: 1817-3195

agreement between simulations and measurements. Moreover, in the DPs, a high level of error was observed for large field sizes (15x15cm² and 20x20cm²) which can be explained by the presence of a high dose gradient in the geometric penumbra which leads to higher relative errors between the experimental and simulated curves (Table 7). Another reason could be the approximation concerning the modeling of the jaws, which amounts to modifying the edges of fields in the transverse profiles as well as the slope in the geometrical penumbra. Finally, the results associated to Sc (figure9) present a good agreement between the simulation code and experiments, which is lower than 1% for all field sizes (Table 8).

TABLE 6: σ AND σ_{max} RESULTS APPLIED TO PDD FOR DIFFERENT FIELD SIZES: 3X3, 4X4, 6X6, 8X8, 10X10(REFERENCE), 12X12, 15X15 AND 20X20 CM².

Field sizes (cm²)	$\lvert\sigma\rvert$(%)	σ_{max} (%)
3x3	0.05	1.66
4x4	0.12	1.28
6x6	0.09	1.12
8x8	0.07	1.33
10x10	0.04	1.28
12x12	0.19	1.66
15x15	0.21	1.58
20x20	0.33	2.81

TABLE 7: σ AND σ_{max} RESULTS APPLIED TO DP FOR DIFFERENT FIELD SIZES: 3X3, 4X4, 6X6, 8X8, 10X10(REFERENCE), 12X12, 15X15 AND 20X20 CM².

Field sizes (cm²)	$\lvert\sigma\rvert$(%)	σ_{max} (%)
3x3	0.12	0.42
4x4	0.19	0.51
6x6	0.25	0.66
8x8	0.29	0.89
10x10	0.33	1.02
12x12	0.98	2.88
15x15	1.02	3.01
20x20	1.92	4.66

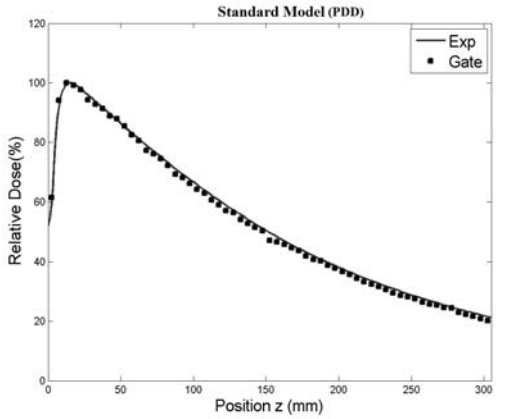

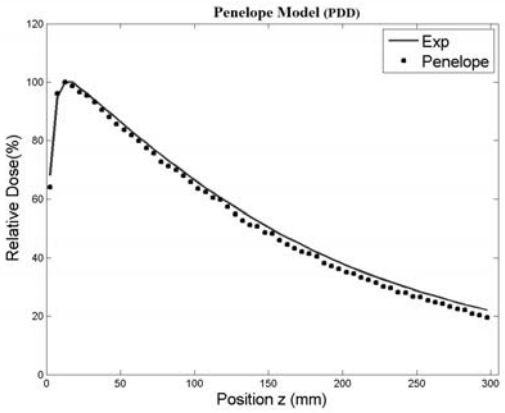

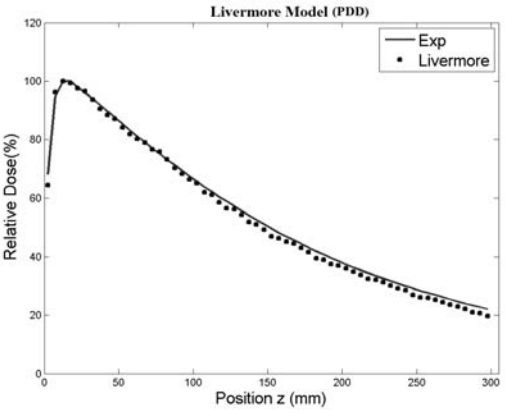

ISSN: 1992-8645 www.jatit.org E-ISSN: 1817-3195

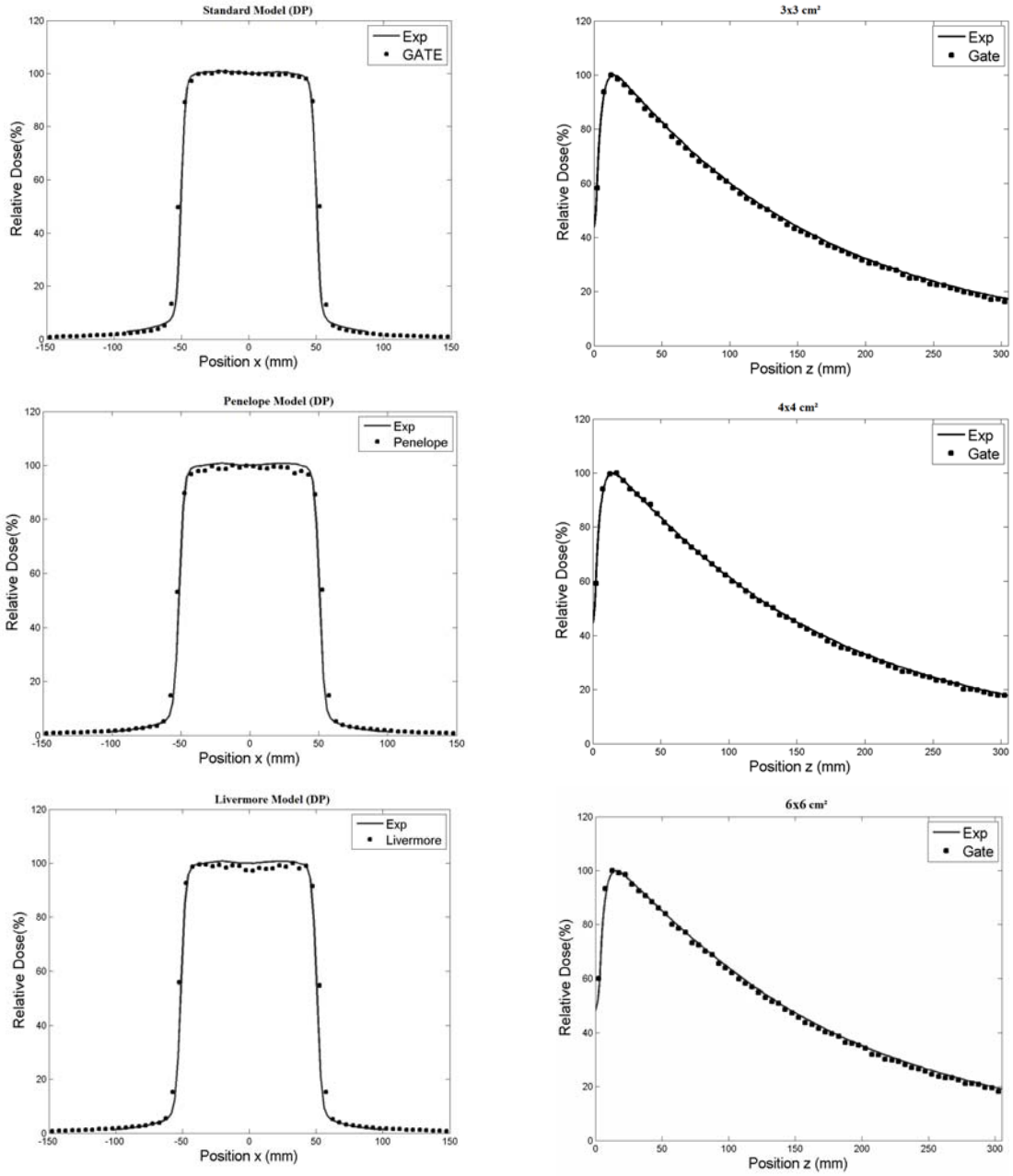

Figure 6: PDDs and DPs for three EM physics models: Standard, Penelope and Livermore.

ISSN: 1992-8645 www.jatit.org E-ISSN: 1817-3195

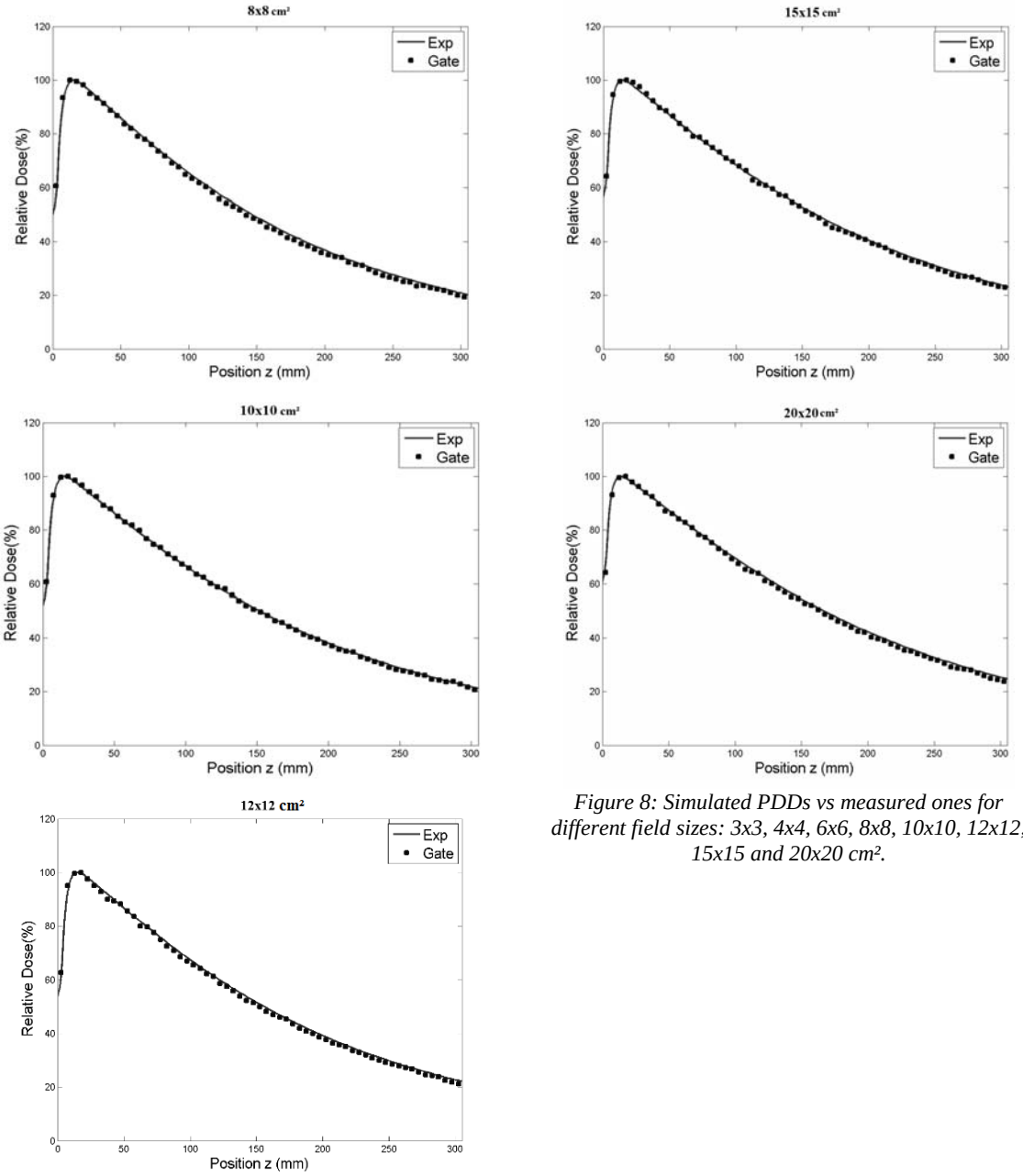

Figure 8: Simulated PDDs vs measured ones for different field sizes: 3x3, 4x4, 6x6, 8x8, 10x10, 12x12, 15x15 and 20x20 cm².

ISSN: 1992-8645 www.jatit.org E-ISSN: 1817-3195

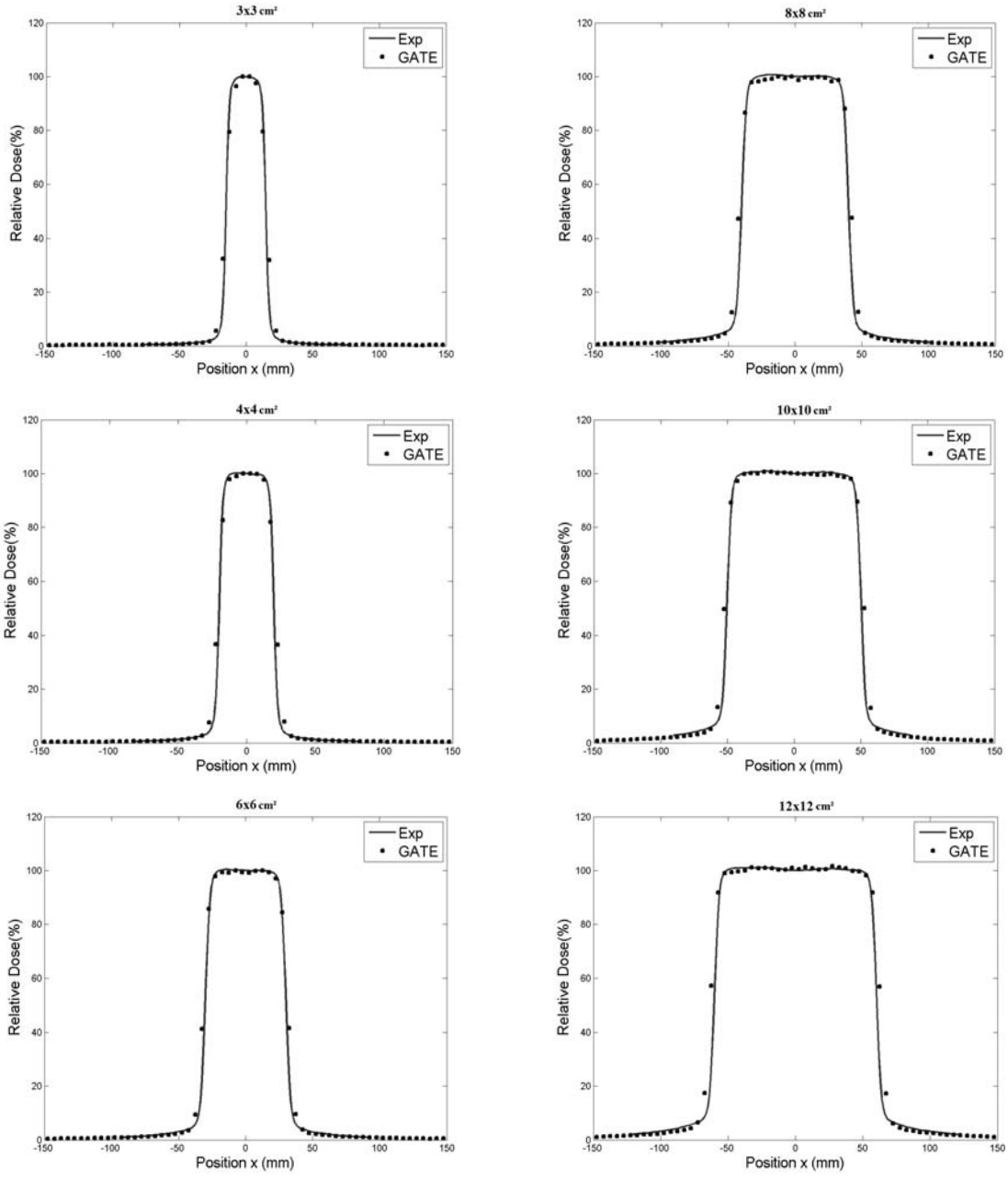

Journal of Theoretical and Applied Information Technology
30th April 2020. Vol.98. No 08

ISSN: 1992-8645 www.jatit.org E-ISSN: 1817-3195

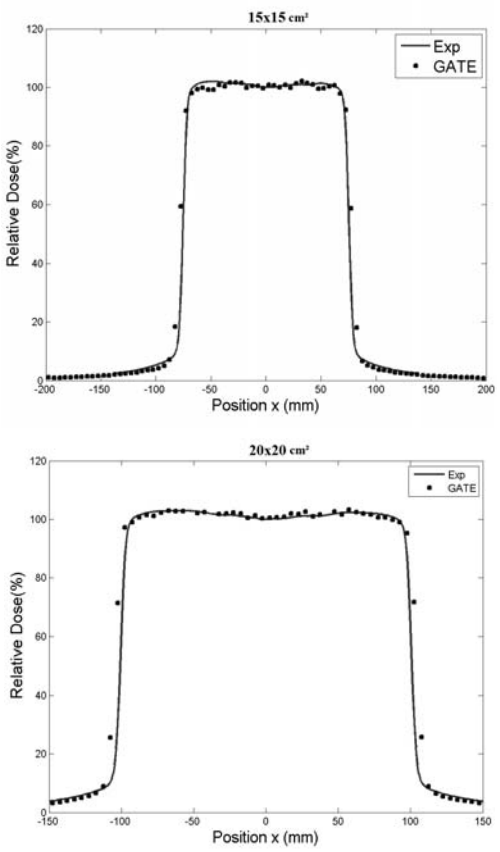

Figure 9: Simulated DPs vs measured ones for different field sizes: 3x3, 4x4, 6x6, 8x8, 10x10, 12x12, 15x15 and 20x20 cm².

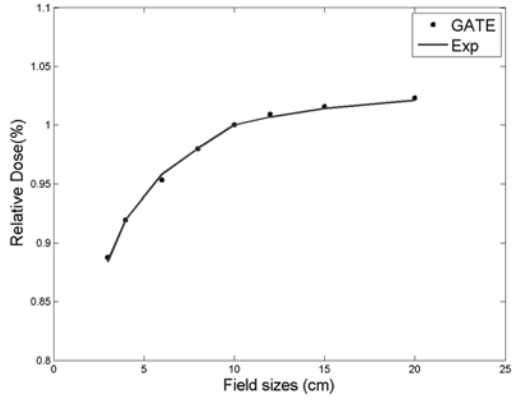

Figure 10: Collimator scatter factor (Sc) at 5cm of depth (reference) for different field sizes: 3x3; 4x4; 6x6; 8x8; 10x10; 12x12; 15x15and 20x20

Table 8: The Average Of Differences ($|\sigma_{Sc}|$) Between Calculated Scs And Measured Ones For Different Field Sizes: 3x3, 5x5, 10x10(Reference) And 20x20 Cm².

Field sizes (cm²)	$\|\sigma_{Sc}\|$(%)
3x3	0.6
4x4	0.12
6x6	0.18
8x8	0.23
10x10	0
12x12	0.33
15x15	0.48
20x20	0.78

4. CONCLUSION

The goal of this study was to investigate the potential of the recent version of GATE code (v8.1) release for radiation therapy to simulate and validate a numerical model of VARIAN Clinac IX against measurements. Compared to previous similar works in the literature [8,10-12]. We have presented the impact of using different physics model in term of dose calculations a CPU timing. Additionally, we have explained the combination of HPC and phase space technic to accelerate the simulations.

In this work, the electron source has been optimized based on the accuracy of geometry elements of the accelerator head and the application of the comparison criteria [8]. After several tests, the suitable configuration was a source beam with an average energy of 5.8 MeV, width at mid-height of 3% and a uniform spatial distribution of 1 mm. Then, calculation time has been optimized essentially by the phase space technique (module1 + module2; A gain factor of about 160 has been reached. Finally, for different field sizes used to validate the numerical model Varian Clinac IX, there were minimal differences between simulation and measurements with deviations below 1% for PDDs (after maximum depth) and DPs (in the horn region).

REFRENCES:

[1] Fippel M. Fast monte carlo dose calculation for photon beams based on the vmc electron algorithm. Med. Phys., 26 :1466–1475, 1999.

[2] Chetty I. J., Curran B., Cygler J. E., DeMarco J. J., Ezzell G., Faddegon B. A., Kawrakow I., Keall P. J., Liu H., Ma C.-M. C., Rogers D. W. O., Seuntjens J., Sheikh-Bagheri D., and Siebers J. V. Report of the aapm task group no. 105: Issues associated with clinical implementation of monte carlo-based photon and electron external beam treatment planning. Med. Phys., 34 :4818–4853, 2007. 85, 157.

ISSN: 1992-8645 www.jatit.org E-ISSN: 1817-3195

[3] da Rosa LA, Cardoso SC, Campos LT, Alves VGL, Batista DVS, Facure A. Percentage depth dose evaluation in heterogeneous media using thermoluminescent dosimetry. J Appl. Clin. Med. Phys. 2010;11(1):117-127.

[4] Bednarz B. Monte Carlo modeling of a 6 and 18 MV Varian Clinac medical accelerator for in-field and out-of-field dose calculations: development and validation. Phys Med Biol. 2009 Feb 21; 54(4): N43–N57.

[5] S. Yani Monte carlo simulation of varian clinac iX 10 MV photon beam for small field dosimetry. Int. J. Radiat. Res., July 2017; 15(3): 275-282.

[6] Hyojun P. Analysis of Dose Distribution According to the Initial Electron Beam of the Linear Accelerator: A Monte Carlo Study.Journal of Radiation Protection and Research 2018;43(1):10-19

[7] Opengate collaboration (2019). GATE UsersGuideV8.1, http://wiki.opengatecollaboration.org/index.php/Users_Guide

[8] Cho S.H., Vassiliev O.N., Lee S., Liu H.H., Ibbott G.S., and Mohan R. Reference photon dosimetry data and reference phase space data for the 6 mv photon beam from varian clinac 2100 serie linear accelerators. Med. Phys., 32 :137–148, 2005.

[9] https://www.marwan.ma/index.php/services/hpc 2018 MARWAN 4

[10] https://www.myvarian.com1999-2018 Varian Medical Systems,

[11] Chetty I J *et al* 2007 Report of the AAPM Task Group no. 105: issues associated with clinical implementation of Monte Carlo-based photon and electron external beam treatment planning *Med. Phys.* **34** 4818–53

[12] Verhaegen F. and Seuntjens J. Monte carlo modelling of external radiotherapy photon beams. Phys. Med. Biol., 48 :R107–R164, 2003.

[13] Keall P, Siebers JV, Libby B, Mohan R. Determining the incident electron fluence for Monte Carlo-based photon treatment planning using a standard measured data set. Medical Physics. 2003; 30(4):574-582.

[14] Sarrut D. and GuiguesL. Region-oriented ct image representation for reducing computing time of monte carlo simulations. Med. Phys., En revision, 2008.

[15] Karzmark, C. J., Craig S. Nunan, and Eiji Tanabe. Medical electron accelerators. 1st edition. New York. McGraw-Hill. 1993.

[16] Geant4 Collaboration, http://geant4-userdoc.web.cern.ch/geant4userdoc/UsersGuides/PhysicsReferenceManual/fo/PhysicsReferenceManual.pdf

[17] Apostolakis, J., S. Giani, et al. (1999). "Geant4 low energy electromagnetics models for electrons and photons." CERN-OPEN-99-034, IFN/AE99/18.

[18] Fix, M. K., P. Manser, et al. (2001). "Monte Carlo simulation of a dynamic MLC based on a multiple source model." Phys Med Biol **46**(12): 18.

[19] Apostolakis J *et al* 2009 Geometry and physics of the Geant4 toolkit for high and medium energy applications *Workshop on Use of Monte Carlo Techniques for Design and Analysis of Radiation Detectors, Radiat. Phys. Chem.* **78** 859–73

[20] Poon E, Verhaegen F, 2005. Accuracy of the photon and electron physics in GEANT4 for radiotherapy applications. Journal of Medical Physics 32, 1696-711.

[21] Lovelock D.M.J., Chui C.S., and Mohan R. A monte carlo model of photon beams used in radiation therapy. Med. Phys., 22 :1387–1394, 1995.

[22] DeMarco J.J., Solberg T.D., and Smathers J.B. A ct-based monte carlo simulation tool for dosimetry planning and analysis. Med. Phys., 25 :1–11, 1998.

[23] Libby B., Siebers J., and Mohan R. Validation of monte carlo generated phase-space descriptions of medical linear accelerator. Med. Phys., 26 :1476–1483, 1999.